THE EFFECT OF ORGANO-NANOCLAY AND PREPARATION METHODS ON CURING KINETICS AND MECHANICAL PROPERTIES OF EPOXY NANOCOMPOSITE

T.-D. Ngo[1*], M.-T. Ton-That[2], K. C. Cole[2], and S. V. Hoa[1]

[1]Department of Mechanical & Industrial Engineering, Concordia University
1455 De Maisonneuve Blvd., Montreal, Quebec, Canada H3G 1M8
[2]National Research Council Canada, Industrial Materials Institute
75 De Mortagne Blvd., Boucherville, Quebec, Canada J4B 6Y4
[*] Faculty of Materials Technology, HoChiMinh City University of Technology
268 Ly Thuong Kiet, Dist. 10, HCM City, Viet Nam

ABSTRACT

The effect of organo-nanoclay (Cloisite 30B) and mixing methods on the cure mechanism, kinetics, and properties of epoxy nanocomposites based on Epon 828 and Epicure 3046 was studied. Two processes were used to prepare the epoxy nanocomposites. The first one is a direct process, in which the clay and epoxy are mixed at room temperature by mechanical mixing. The second one is a high temperature process, in which the clay and epoxy are mixed at 120°C for 1 hour. The heat evolution of the epoxy resin formulation and its nanocomposite systems was measured during dynamic DSC scans at heating rates of 2.5, 5, 10, 15, and 20°C·min^{-1}. The cure kinetics of these systems was modelled by means of different approaches. Kissinger and isoconversional models were used to calculate the kinetics parameters while the Avrami model was utilized to compare the cure behavior of the systems. The presence of Cloisite 30B and the mixing method both had an effect on the cure kinetics and mechanical properties of the epoxy system.

Key words: *nanoclay, epoxy, nanocomposites, cure kinetics, DSC, mechanical properties*

1. INTRODUCTION

Clay nanolayers have been shown to be very effective reinforcements in epoxy systems [1-3]. Hydrophilic clay is not highly compatible with the epoxy matrix, resulting in poor dispersion and a weak interface. To improve the interfacial interaction between the nanoclay and the matrix, surface modification of the nanoclay by organic compounds (so-called "intercalants") is essential. The most popular intercalants are compounds based on onium ions, which contain an amine cation and a long hydrocarbon chain. The presence of intercalant may affect the curing process in terms of chemistry, while the presence of clay platelets at an atomic scale may inhibit the curing reaction through a steric effect of the clay. The effect of primary-amine based intercalant on the polymerization of epoxy has been described by Lan et al. [4] but there have been few investigations on the impact of such effects on the mechanism and kinetics of the curing process. In addition, a steric effect of clay on the curing of intercalated epoxy matrix has been discussed by Kornmann et al. [5, 6].

Our previous study [7] investigated the kinetics and steric effects of another organo-clay (Nanomer I.30E = octadecyl-amine-modified montmorillonite) on the cure of the nanocomposite. The activation energy and the Avrami exponent are important indices for the cure analysis, while the simulation of the cure process is an important prerequisite component in establishing the relationship between

processing and properties of epoxy systems and their nanocomposites based on Nanomer I.30E. The activation energy of the epoxy nanocomposite is similar to that of the epoxy-amine system in the early stages of dynamic DSC cure (i.e. at lower temperature), but is substantially lower in the later stages (at higher temperature). The presence of nanoclay facilitates the curing reaction, especially the etherification reaction (as opposed to the initial epoxy-amine reaction). On the other hand, the Avrami approach indicated a steric effect of the exfoliated clay on the cure of the nanocomposite.

The aim of this work is to understand the effect of the organo-nanoclay Cloisite 30B (a natural montmorillonite modified with a quaternary ammonium salt) and mixing methods on the cure mechanism, kinetics and properties of epoxy nanocomposites in which the nanoclay has been exfoliated or intercalated in the matrix.

2. EXPERIMENTAL

2.1 Materials

An organo-nanoclay recommended for amine-cured epoxy systems, Cloisite 30B from Southern Clay Products, Inc. was used in this study. It consists of montmorillonite treated with methyl tallow bis-(2-hydroxyethyl) quaternary ammonium.

The resin and hardener selected for this study were Shell Epon 828 and Shell Epicure 3046, respectively. Samples were cured either at room temperature for 2 days or at 120°C for 1 hour, with subsequent post cure at 140°C for 2 hours in both cases.

2.2 Sample Preparation

In this work, two processes were used to prepare the epoxy nanocomposites. The first one (Method 1) is a direct process, in which the clay and epoxy are mixed at room temperature by mechanical mixing; the nanoclay content in the epoxy resin in this case was 2 phr. The second one (Method 2) is a high temperature process, in which the clay and epoxy are mixed at 120°C for 1 hour; the nanoclay content in the epoxy resin in this case was 2 and 4 phr. Sample specifications are shown in Table 1.

Table 1. Sample specifications

Designation	Epon 828	Epicure 3046	Cloisite 30B	Mixing method
8EP	100	35	0	-
8EP-2pB-M1	100	35	2	Method 1
8EP-2pB-M2	100	35	2	Method 2
8EP-4pB-M2	100	35	4	Method 2

2.3 Measurements

The DSC data were obtained on a Perkin-Elmer Pyris 1 instrument using nitrogen atmosphere. The samples were heated from 30°C to 250°C (dynamic scan) at five different heating rates (2.5, 5, 10, 15, and 20°C·min^{-1}) to follow the heat evolution due to the chemical reaction occurring in this temperature range. The cured sample was then cooled to 30°C at 20°C·min^{-1} to minimize the enthalpy relaxation in the second heating scan. Finally, the sample was reheated to 250°C at 20°C·min^{-1} in order to determine the glass transition temperature (T_g) and the post curing reaction if any.

To evaluate the dispersion of the nanoclay in the polymer matrix, X-ray diffraction patterns were obtained from the surface of the samples with a Bruker Discover 8 powder X-ray diffractometer with CuKα radiation. The experiments were conducted on the exposed surface of specimens prepared by casting. A Hitachi-S4700 scanning electron microscope

(SEM) was used to observe the dispersion of clay in the epoxy matrix.

The flexural and tensile properties of the epoxy and epoxy nanocomposites were performed on Instron 5500R system at room temperature and 50% relative humidity according to ASTM D790-2000 and ASTM D638-2002, with crosshead speeds of 1.3 mm/min and 5 mm/min, respectively.

3. RESULTS AND DISCUSSION

3.1 Dispersion

X-ray diffraction curves of the epoxy system and its nanocomposites based on Cloisite 30B are illustrated in Figure 1. The d-spacing data calculated therefrom are summarized in Table 2. In all the nanocomposite samples the clay layer separation (intercalation) is considerably higher than in the original Cloisite 30B. There is no significant difference between the clay loading levels of 2 phr and 4 phr. However, at the same loading level of 2 phr, the 8EP-2pB-M2 (epoxy and clay mixed at high temperature) shows better intercalation than 8EP-2pB-M1 (epoxy and clay mixed at room temperature), whether the samples were cured at room temperature or at 120°C. For instance, when samples were cured at room temperature, the d-spacing of 8EP-2pB-M2 is 4.23 nm, compared with 3.99 for 8EP-2pB-M1. A high temperature of mixing speeds up the diffusion of the polymer into the clay galleries.

In addition, the X-ray results also indicate that the curing of the nanocomposites at the higher temperature of 120°C in all cases results in better intercalation than the curing at room temperature for the nanocomposites with the same clay loading and mixing method. The X-ray diffraction peak (see Figure 1) shifts to lower angle, which means the degree of delamination increases in all cases. Thus a high curing temperature accelerates the diffusion of the polymer and hardener into the clay galleries [6].

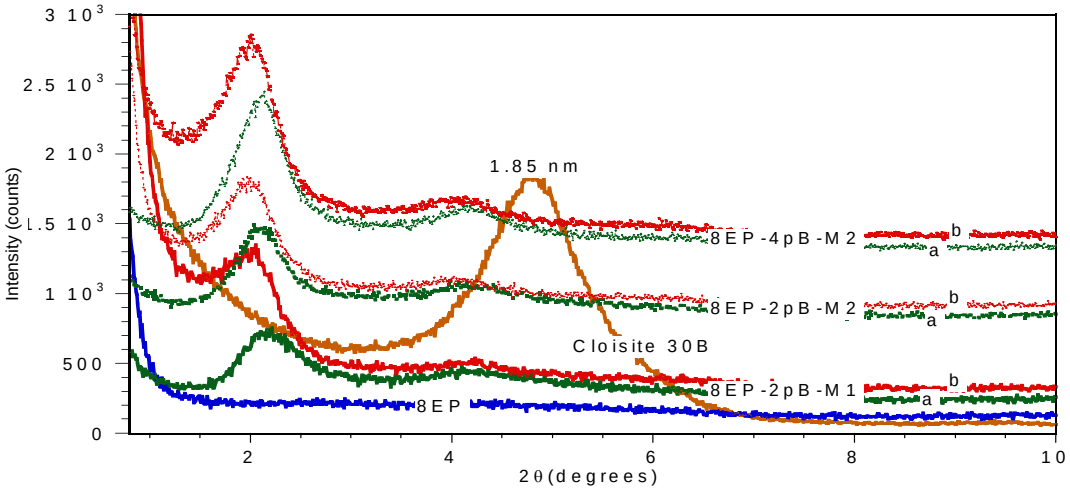

Figure 1. X-ray spectra of the 8EP and its Cloisite 30B nanocomposites: (a) samples cured at room temperature; (b) samples cured at 120°C for 2 h.

Table 2. Summary of XRD data

Sample	Gallery distance (nm)	
	Cured at room temperature	Cured at 120°C for 2 h
8EP	-	
Cloisite 30B	**1.85**	
8EP-2pB-M1	3.99	4.38
8EP-2pB-M2	4.23	4.48
8EP-4pB-M2	4.17	4.41

Figure 2 presents the microstructures of three nanocomposite samples observed by SEM. The bright spots on the backscattered images correspond to clay aggregates. Apparently, at the same loading level of 2 phr, the clay particles are more finely dispersed in the nanocomposite that was prepared at high temperature (8EP-2pB-M2, Figure 2b) compared with room temperature (8EP-2pB-M1, Figure 2a). Moreover, with the same mixing method at high temperature, when the clay loading increases from 2 phr to 4 phr (Figure 2c), the number of aggregates increases. However, this method still shows a better dispersion of clay as compared with mixing at room temperature. The size of clay particles whether in 8EP-2pB-M2 or 8EP-4pB-M2 is smaller than in 8EP-2pB-M1. A high temperature of mixing has a positive effect on the dispersion of the clay in the materials

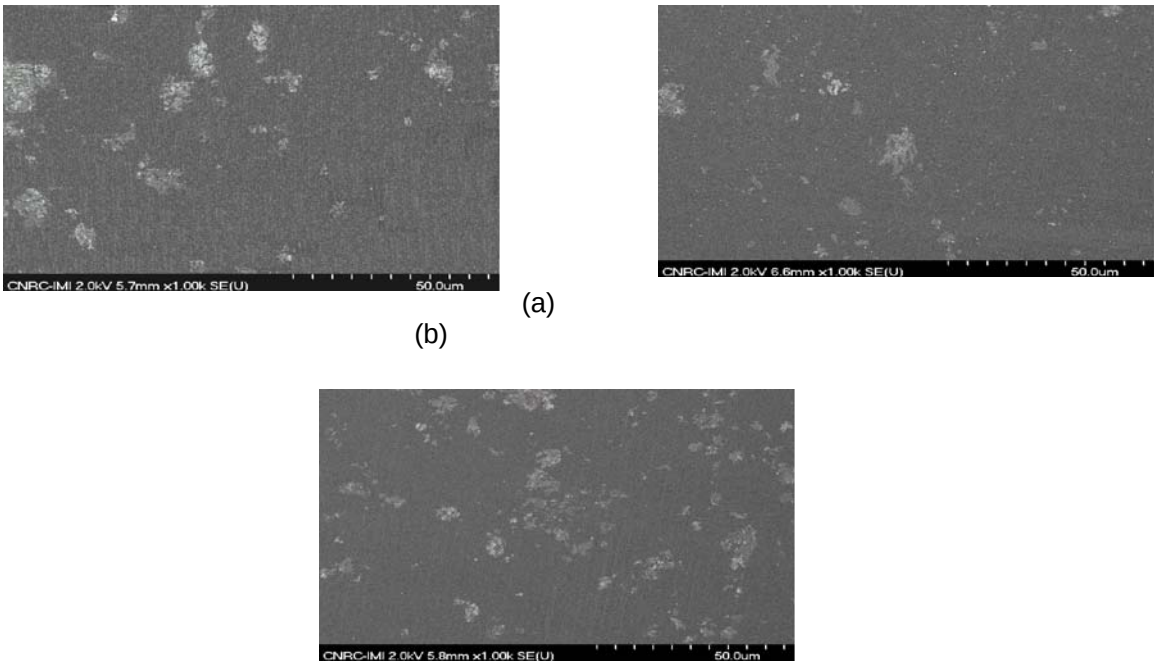

Figure 2. SEM micrographs of (a) 8EP-2pB-M1, (b) 8EP-2pB-M2, (c) 8EP-4pB-M2

3.2 Cure behaviour

DSC curves of the epoxy-amine system and its nanocomposite at different heating rates are shown in Figure 3. The presence of nanoclay has some effect on the curing process as reflected by the difference in the DSC curves of the epoxy and its nanocomposite. This difference is more apparent at lower heating rates than at higher ones.

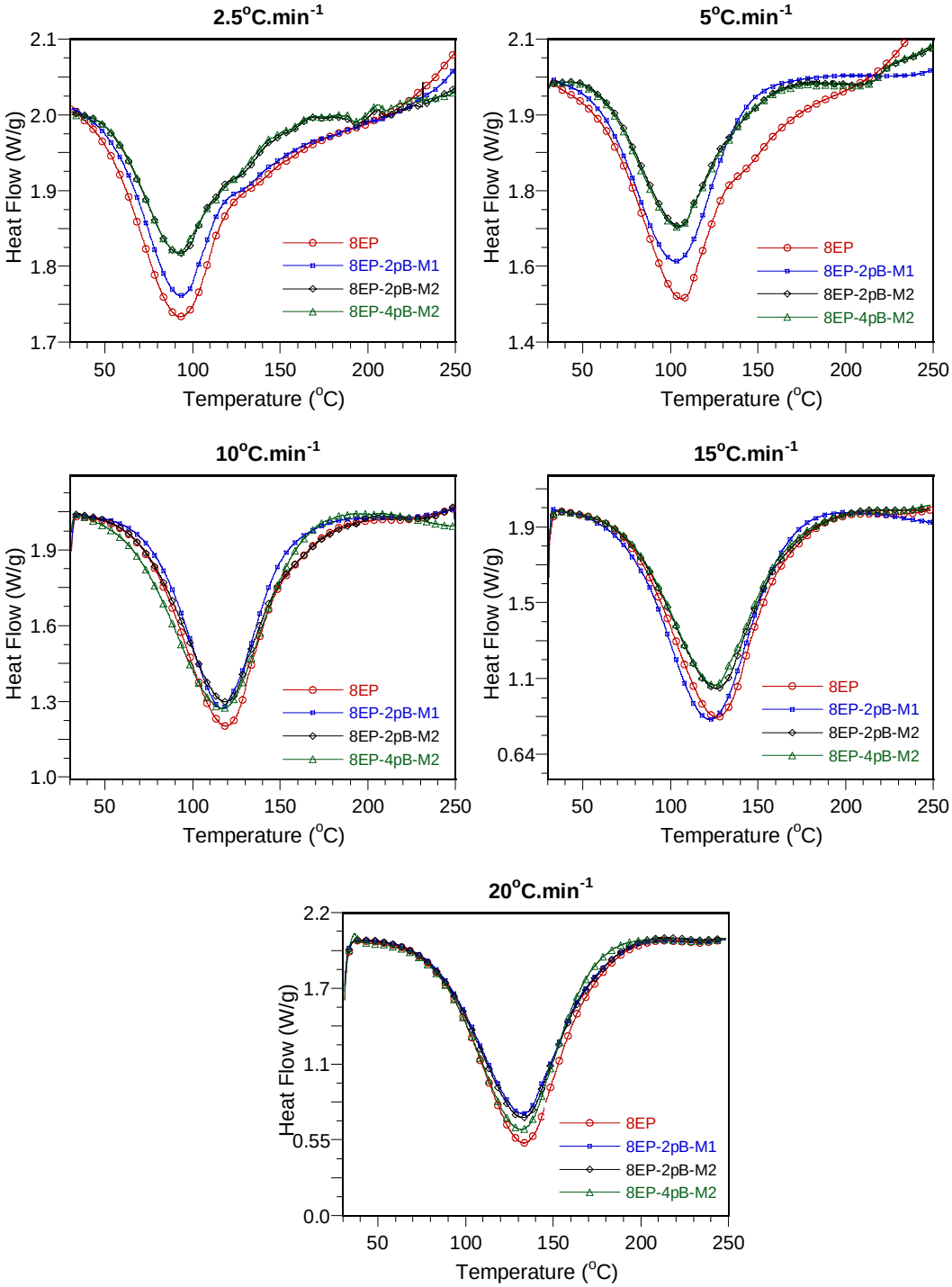

Figure 3. DSC curves of the epoxy-amine system and its nanocomposite at different heating rates.

The mixing method also affects the curing process. At the same clay loading of 2 phr (based on epoxy resin), the DSC curves of the epoxy nanocomposite in which clay and epoxy were mixed at high temperature are different from those of epoxy and epoxy nanocomposite in which clay and epoxy were mixed at room temperature (system 8EP, 8EP-2pB-M1 and 8EP-2pB-M2). This may be caused by the presence of clay and the level of dispersion of clay in the epoxy (see Figure 3 at heating rates 2.5 and 5°C·min^{-1}).

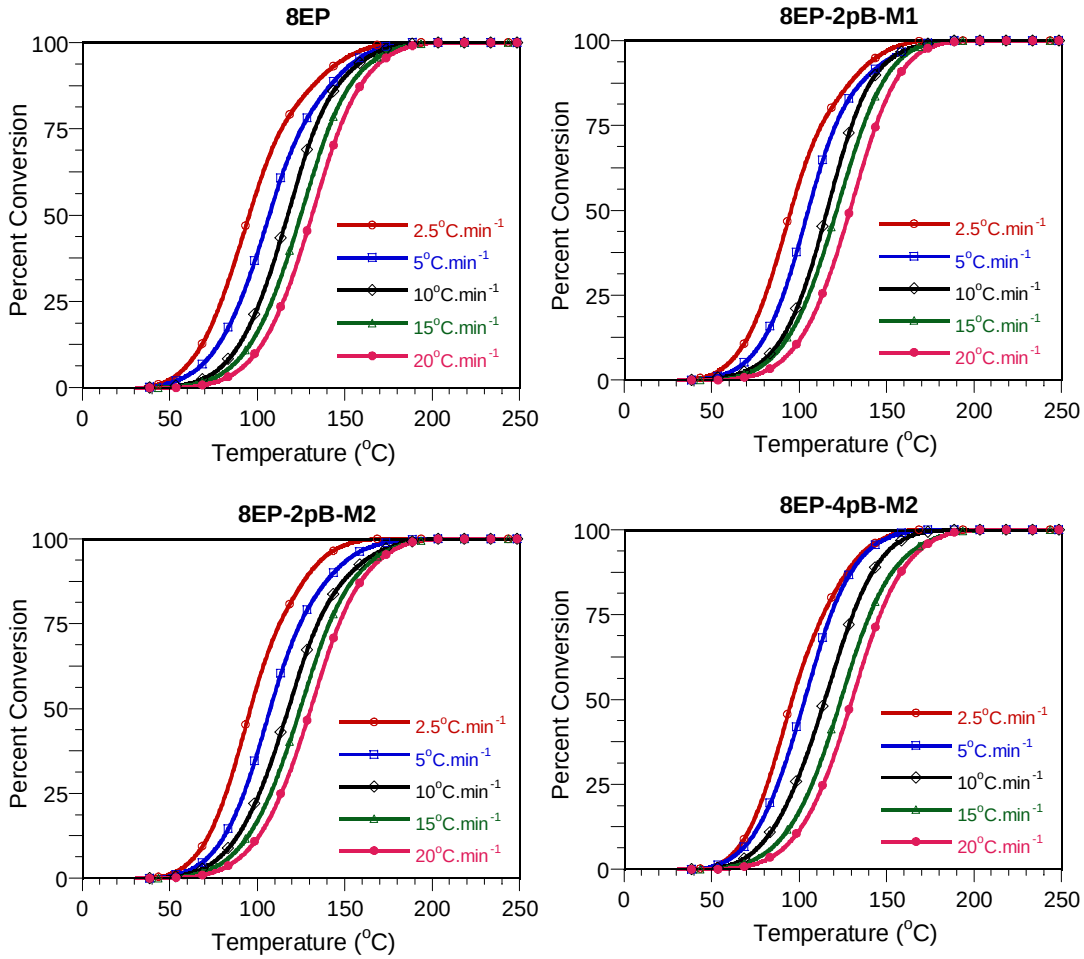

Figure 4. Transformation curves of 8EP and its nanocomposites based on Cloisite 30B at different heating rates.

The transformation curves derived from the DSC results are shown in Figure 4. Generally speaking, the reaction onset and completion occur at lower temperatures at lower heating rates, as can be seen from the T_{onset} values given in Table 3. There is no significant difference between the systems with respect to the T_{onset}, nor with respect to T_p (the temperature of the peak maximum in the heat flow curves). The curing of epoxy with amine involves several different reactions, and the rates of these reactions will vary with temperature in different ways. Thus a change in the heating rate may favour one reaction with respect to another and change the structure of the crosslinked molecular network. This could explain the decrease in the ultimate T_g observed for systems on increasing the heating rate (Table 3), as well as the variations in ΔH. However, it appears that the presence of Cloisite 30B has negligible effect on the matrix T_g

.

Table 3. Curing characteristics for the E828-EP mixture and its nanocomposites.

q (°C·min^{-1})	T_{onset} (°C)	T_p (°C)	ΔH (W/g)	T_g (°C)
8EP				
2.5	51.4	92.9	382.0	87.7
5	59.2	106.3	351.0	86.8
10	69.9	119.0	268.1	79.2
15	74.7	126.7	272.9	73.9
20	81.6	133.3	257.2	72.7
8EP-2pB-M1				
2.5	54.8	93.0	368.0	87.4
5	60.2	103.8	274.9	83.8
10	69.7	116.5	258.6	76.6
15	75.2	123.2	239.0	72.4
20	81.8	131.7	222.9	71.6
8EP-2pB-M2				
2.5	53.0	93.4	273.3	87.5
5	60.7	104.6	267.6	86.3
10	69.5	118.5	276.3	77.5
15	76.1	126.5	270.0	71.9
20	80.8	132.7	264.5	71.0
8EP-4pB-M2				
2.5	54.9	92.0	237.3	87.2
5	62.0	105.2	208.2	85.9
10	71.6	117.2	273.8	77.1
15	76.6	125.5	232.6	74.7
20	83.3	132.1	215.2	73.0

3.3 Activation Energy

The Kissinger analysis is based on the relationship between the heating rate q and the temperature T_p corresponding to the peak in the heat release curve. Activation energy is commonly evaluated by one of two methods: the Kissinger equation or the isoconversional equation.

From the Kissinger equation, only an overall activation energy can be calculated [8]. For nonisothermal curing, the relationship between activation energy E, the heating rate q, and the temperature T_p at which the exothermic peak has its maximum can be described as:

$$E = -R\frac{d(\ln(q/T_p^{\,2}))}{d(T_p^{\,-1})} \qquad (1)$$

where R is the gas constant, equal to 8.3144 J·K^{-1}·mol^{-1}. From the dynamic DSC curves measured at different heating rates, the relation between ln (q/T_p^2) and T_p^{-1} can be obtained,

and then the activation energy can be calculated from the slope [8].

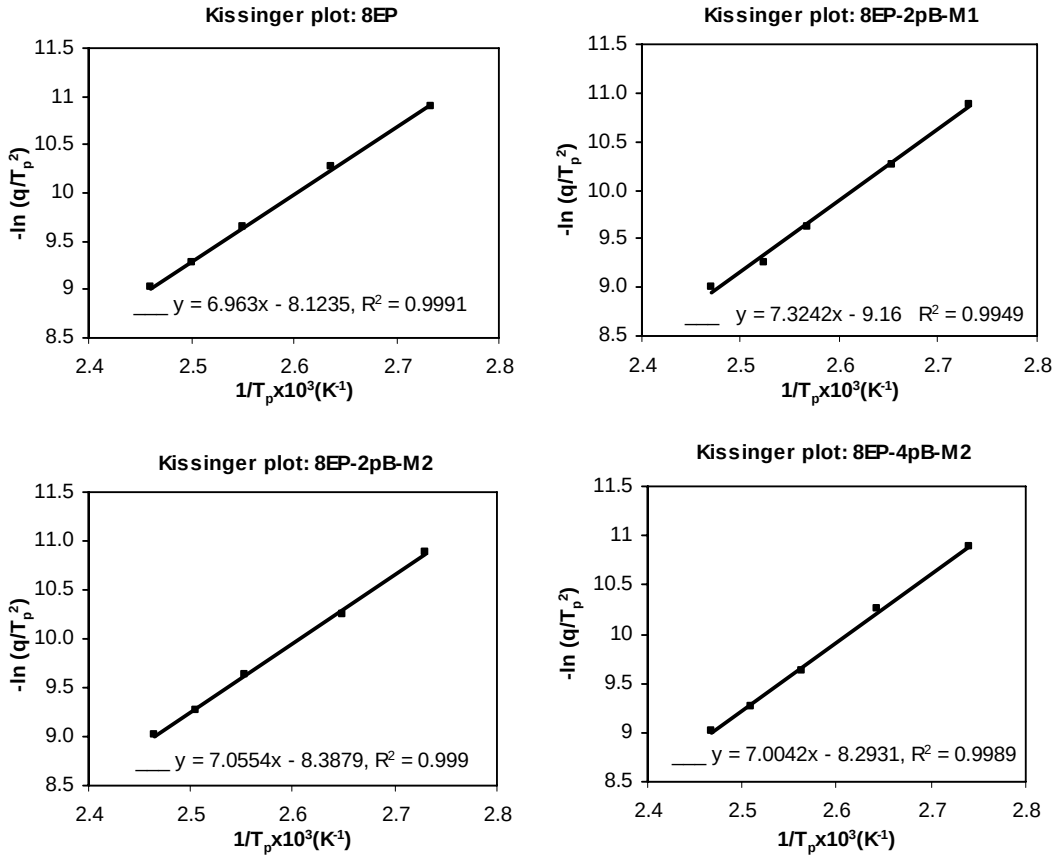

Figure 5. Kissinger plots for the 8EP system and its nanocomposites based on Cloisite 30B.

Figure 5 shows the relationship between ln $(q.T_p^{-2})$ and T_p^{-1} for both the epoxy-amine system and its nanocomposites. The five points correspond to the five heating rates of 2.5, 5, 10, 15, and 20°C·min^{-1}. There is an excellent linear fit in all cases, indicating that the experimental data fit the Kissinger model quite well. From the slopes of these plots the overall activation energy values for epoxy-amine and nanocomposites were calculated and are shown in Table 4. The apparent very slight increase in E_a for the nanocomposites suggests that the positive effect of the organic intercalant to promote the chemical reaction is weaker than the negative impact of the steric effect of the intercalated/exfoliated clay.

Table 4. Activation energy for E828-EP and its nanocomposites from Kissinger analysis.

System	Activation energy (kJ·mol^{-1})
8EP	57.9
8EP-2pB-M1	60.9
8EP-2pB-M2	58.7
8EP-4pB-M2	58.2

The isoconversional analysis is based on the relationship between the heating rate q and the temperature T at which a certain degree of conversion is reached. Unlike the Kissinger approach, the isoconversional approach makes it possible to determine the activation energy corresponding to different stages of cure throughout the entire conversion [8, 9]. The equation used is:

$$E = -R\frac{d(\ln q)}{d(T^{-1})} \qquad (2)$$

where T is the temperature corresponding to a selected degree of conversion α at a given heating rate q. From the slope of a plot of ln q vs. T^{-1} for a chosen degree of conversion, the activation energy corresponding to that degree of conversion can be obtained.

Figure 6 shows the relationship between ln q and T^{-1} for nine different degrees of conversion ranging from 0.1 to 0.9. The linear relationship observed in all cases indicates that the approach is applicable for this case. The activation energies E_a calculated for the four systems are given in Figure 7. Some differences are clearly apparent. For the epoxy-amine system without clay, E_a increases steadily with the degree of cure, particularly in the later stages ($\alpha > 0.7$). When 2 wt% Cloisite 30B is mixed in by Method 1 (room temperature, 8EP-2pB-M1), E_a behaves in a similar manner except that the values are consistently somewhat higher. Thus, even when not well dispersed, the clay appears to have an effect. However, when the clay is better dispersed (high temperature), whether at 2 or 4 wt % (8EP-2pB-M2 and 8EP-4pB-M2), the shape of the E_a vs. α curve changes considerably. The E_a decreases slightly as α increases in the initial stages of cure, then levels off, then rises towards the end, but not nearly as much as when the clay is absent or less well dispersed. It is obvious that the mixing method affects the E_a.

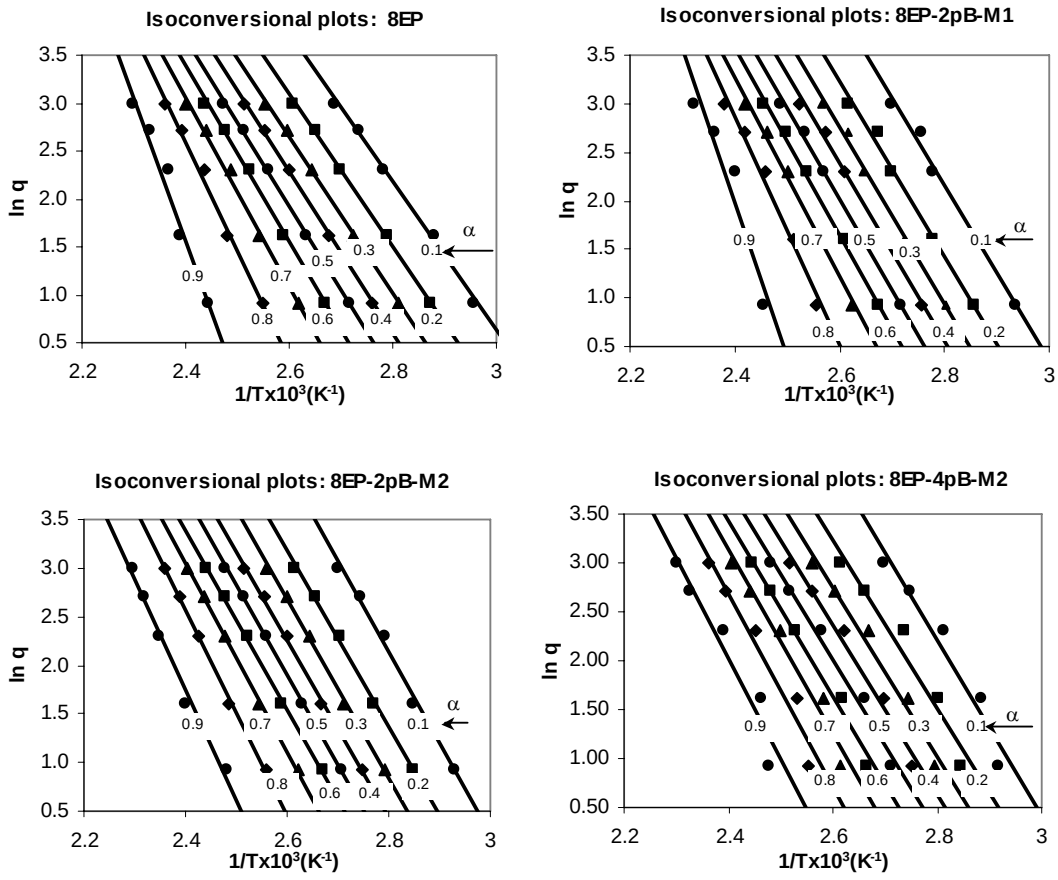

Figure 6. Isoconversional plots at various conversions for the 8EP system and its nanocomposites based on Cloisite 30B.

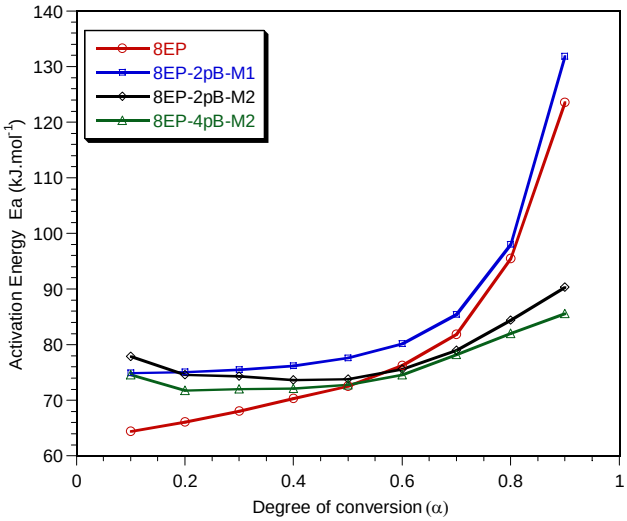

Figure 7. Activation energies obtained for the isoconversional model.

Table 5. Average activation energies obtained for the isoconversional model.

System	Average activation energy ($kJ \cdot mol^{-1}$)
8EP	79.9
8EP-2pB-M1	86.1
8EP-2pB-M2	78.2
8EP-4pB-M2	76.0

The activation energies obtained by the Kissinger approach (Table 4) are lower than the average values obtained by the isoconversional approach (Table 5). This can be explained by the differences in assumptions and mathematical approach between the two models. The isoconversional results are more meaningful than the Kissinger ones because the evolution of the chemistry of the system during the cure is partially taken into account. The Kissinger approach is based entirely on the maximum rate of cure, which occurs in this case around the beginning of the curing reaction [7]. Thus it is not surprising that the E_a values obtained by the Kissinger approach are closer to those obtained at lower degrees of cure by the isoconversional approach rather than to the average isoconversional values.

3.4 Avrami Analysis

From the DSC results, curves of ln[-ln(1-α)] vs. *T* were plotted for two different conversion ranges, namely 0-10% and 10-25%. A linear fit in each range gave the parameters *a* and T_q in Eq. 3 [9]:

$$\ln[-\ln(1-\alpha)] = a\,(T - T_q) \qquad (3)$$

where *a* and T_q are constants. The results for the five different heating rates *q* were then used to make plots of T_q vs. *(*ln *q)/a* according to Eq. 4:

$$T_q = n\frac{\ln q}{a} + T_1 \qquad (4)$$

where the slope is the Avrami exponent and the intercept T_1 corresponds to the T_q at q = 1 K·min^{-1}.

The results are shown in Figures 8 and 9. The Avrami exponents n obtained from the slopes are given in Table 6. For both epoxy-amine and nanocomposites, the Avrami exponent n in the early stage of cure is greater than in the second stage. It can be understood that at low conversions, the concentration and the size of the microgels are still small, and their growth is less space-restricted. With the advancement of cure the number of microgels and their size increases, so their growth is restrained and inter-microgelation may occur. When the cure reaches its end, intermicrogelation becomes dominant, a three-dimensional network is formed, and the reaction nearly stops [7].

Table 6. Exponents n obtained from Avrami analysis.

System	α = 0-10%	α = 10-25%
8EP	1.27	1.09
8EP-2pB-M1	1.33	1.07
8EP-2pB-M2	1.30	0.97
8EP-4pB-M2	1.26	1.02

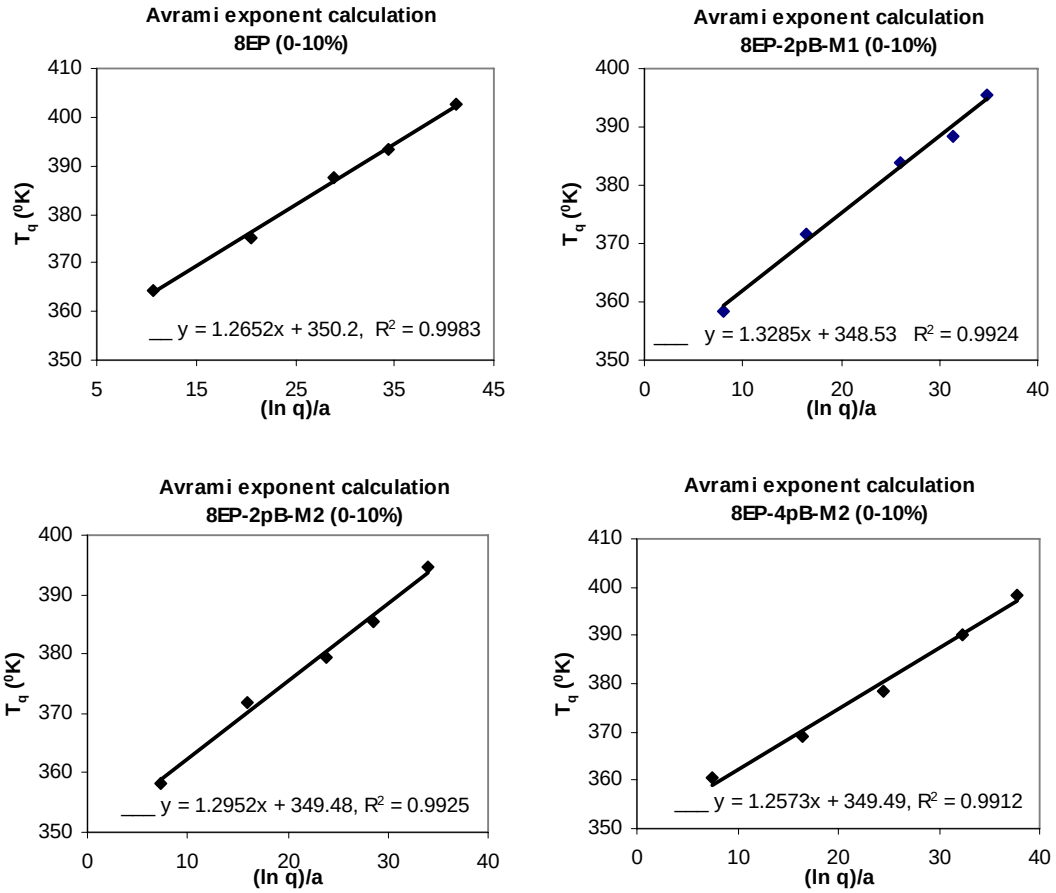

Figure 8. Determination of the Avrami exponent n for the epoxy-amine system and its nanocomposites with α = 0-10%.

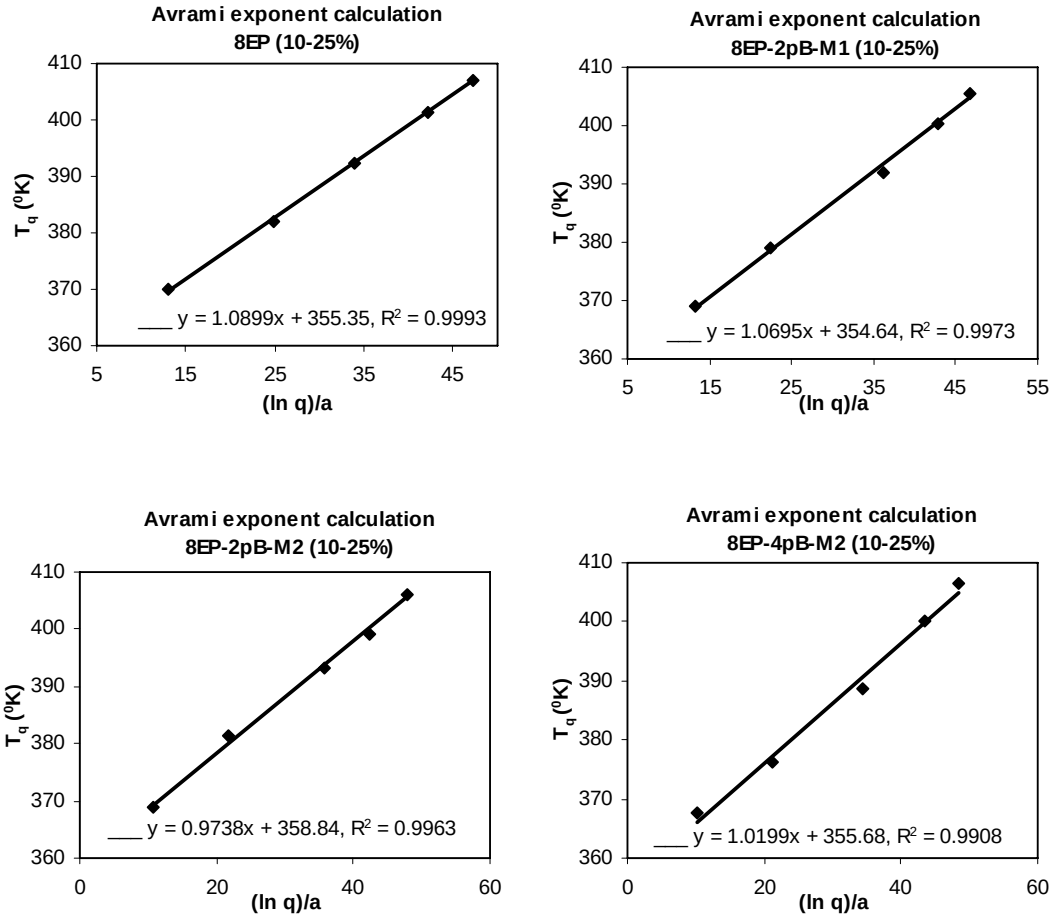

Figure 9. Determination of the Avrami exponent n for the epoxy-amine system and its nanocomposites with α = 10-25%.

The long polymer chains tend to form spherical structures (so-called "microgels") with high cyclization and crosslinking density after the initial period of polymerization [10, 11]. The number of microgels increases during the early stages. The epoxy and hydroxyl groups of the epoxy resin and the amine groups of the hardener within the microgels continue to react to improve the crosslinking density, while those near the surface react with surrounding monomers and oligomers, leading to increased microgel diameter and microgel interconnection. The Avrami exponent reflects the steric freedom of microgel growth. A higher n value indicates greater freedom of growth, and a change of *n* value during the cure indicates a marked change in polymerization mechanism [7].

3.5 Mechanical Properties

Figures 10 and 11 provide the tensile and flexural properties of 8EP and its nanocomposites. The presence of Cloisite 30B results in an increase in modulus, whether in tension or flexion. Since clay has a much higher modulus than the epoxy matrix, it is easy to understand, based on the rule of mixtures, why the modulus of the nanocomposites can be improved by adding nanoclay. However, the strength of the materials is dependent not only on the dispersion of the clay in the matrix but also on the quality of the interface between clay and matrix as well as the structure of the materials. As confirmed by X-ray diffraction, mixing at higher temperature gives a better dispersion of nanoclay in epoxy as compared with mixing at room temperature. This explains why, at the

same 2 phr level of nanoclay, the 8EP-2pB-M2 sample in which the epoxy and clay were mixed at high temperature (M2) gives higher strength than 8EP-2pB-M1 in which the epoxy and clay were mixed at room temperature (M1).

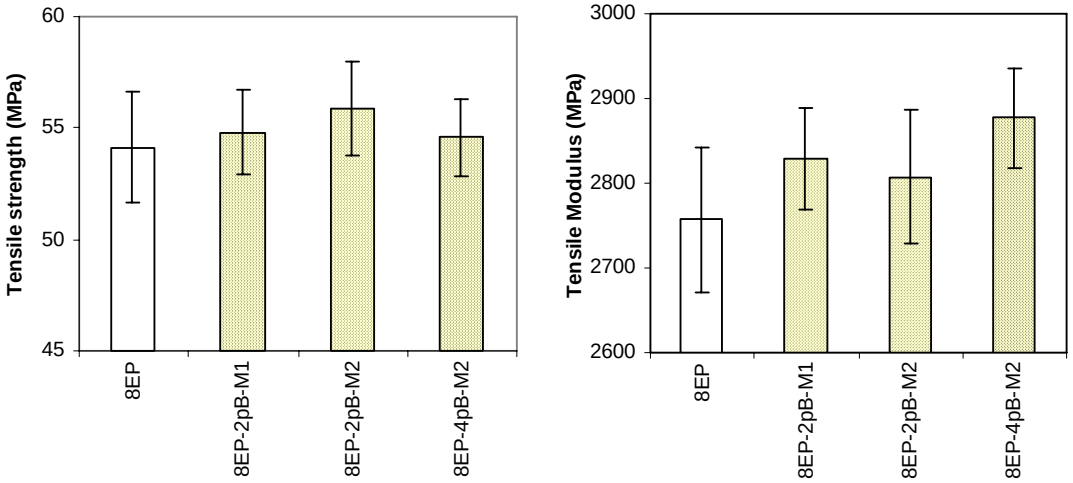

Figure 10. Tensile properties of 8EP and its nanocomposites

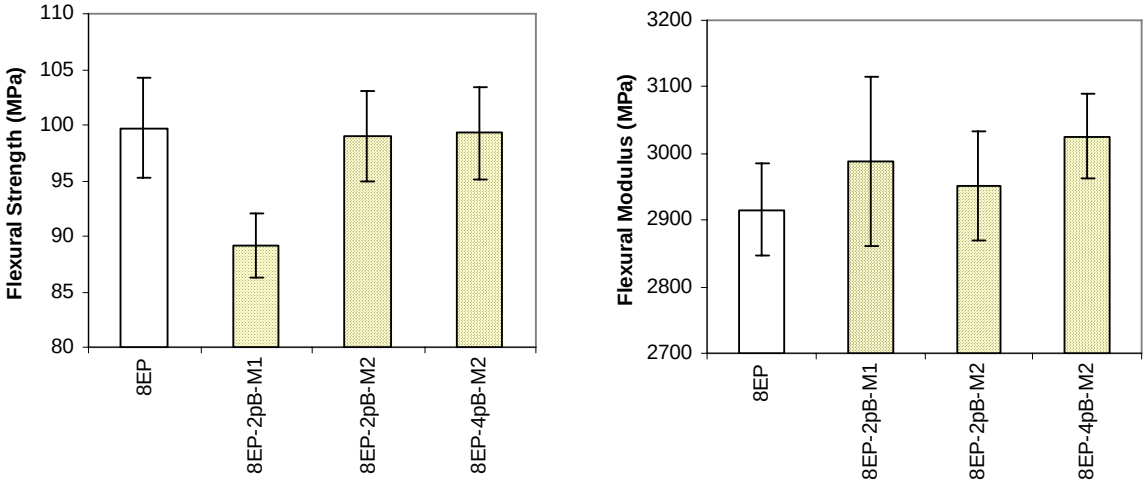

Figure 11. Flexural properties of 8EP and its nanocomposites

4. CONCLUSION

There is a difference in cure kinetics between the epoxy nanocomposites based on Cloisite 30B nanoclay and the corresponding epoxy-amine system without clay. Generally speaking, the activation energy E_a increases more or less steadily as a function of the degree of cure. The E_a of the mixture containing poorly dispersed clay (mixed at room temperature) is somewhat higher than that of epoxy-amine at all stages of dynamic DSC cure. For systems mixed at high temperature, E_a is higher in the early stages of cure (i.e. at lower temperature) and lower in the later stages (at higher temperature). On the other hand, the Avrami approach indicates a steric effect of the intercalated/exfoliated clay on the cure of the nanocomposite. The use of these two approaches provides a better

understanding of the cure kinetics and mechanism of the nanocomposite formation. Thus the presence of nanoclay and the mixing method both affect the cure kinetics and mechanical properties of epoxy nanocomposite.

Further work involving structure and isothermal cure is underway to more clearly establish the kinetic models for the cure of this epoxy system and its nanocomposites.

5. ACKNOWLEDGEMENTS

We acknowledge the Vietnamese Government for a studentship to T.-D. Ngo. We also thank the National Science & Engineering Research Council of Canada for funding in this project.

REFERENCES

1. P. B. Messersmith and E. P. Giannelis, *Chem. Mater*., **6**, 1719 (1994).
2. T. Lan and T. J. Pinnavaia, *Chem. Mater*., **6**, 2216 (1994).
3. J. Massam and T. J. Pinnavaia, *Mater. Res. Soc. Symp. Proc.* **520**, 223 (1998).
4. T. Lan, P. D. Kaviratna, and T. J. Pinnavaia, *J. Phys. Chem. Solids*, **57**, 1005 (1996).
5. X. Kornmann, H. Lindberg, and L. A. Berglund, *Polymer*, **42**, 1303 (2001).
6. X. Kornmann, H. Lindberg, and L. A. Berglund, *Polymer*, **42**, 4493 (2001).
7. M.-T. Ton-That, T.-D. Ngo, P. Ding, G. Fang, K. C. Cole, S. V. Hoa, *Polym. Eng. Sci.*, **44**, 1132 (2004).
8. F. Y. C. Boey and W. Qiang, *Polymer*, **41,** 2081 (2000).
9. K. P. Chuah, S. N. Gan, and K. K. Chee, *Polymer*, **40**, 253 (1998).
10. S. V. Muzumdar and L. J. Lee, *Polym. Eng. Sci.*, **36**, 943 (1996).
11. M. G. Lu, M. J. Shim, and S. W. Kim, *Thermochim. Acta*, **323**, 37-42 (1998).